

# Cumyl Dithiobenzoate Mediated RAFT Polymerization of Styrene at High Temperatures

Toshihiko Arita, Michael Buback, and Philipp Vana\*

Institut für Physikalische Chemie, Georg-August-Universität Göttingen,  
Tammannstr. 6, D-37077 Göttingen, Germany

Received May 17, 2005; Revised Manuscript Received July 21, 2005

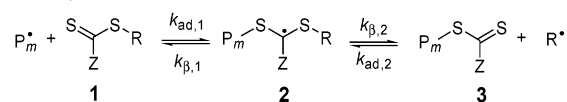
**ABSTRACT:** Self-initiated reversible addition fragmentation chain transfer (RAFT) polymerizations of styrene at temperatures of 120, 150, and 180 °C, using cumyl dithiobenzoate (CDB) at concentrations between  $5.0 \times 10^{-3}$  and  $2.0 \times 10^{-2}$  mol L<sup>-1</sup> as the RAFT agent were performed at 1000 bar. The increase of average molecular weight with monomer conversion, the shape of the molecular weight distributions, and polydispersity indices below 1.5 at monomer conversions up to about 50% indicate control of styrene bulk polymerization even at the high experimental temperatures. Neither a substantial decomposition of the RAFT agent nor a change in the overall polymerization process, e.g., by ionic side reactions, is observed. Polymerization rates are lower than in conventional styrene polymerization. The rate retardation effect increases with CDB concentration but is clearly reduced toward higher temperature. The lower retardation effect at high temperatures is assigned to a lower equilibrium concentration of the intermediate RAFT radical. The experimental rate data can be consistently described in terms of the concept of irreversible termination of the intermediate RAFT radical. On the other hand, the data are qualitatively and semiquantitatively inconsistent with the idea of slow fragmentation of intermediate radicals. The analysis of the kinetic data results in a reaction enthalpy of about 50 kJ mol<sup>-1</sup> for the  $\beta$ -scission reaction of the intermediate RAFT radical.

## Introduction

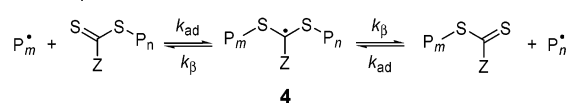
Reversible addition fragmentation chain transfer (RAFT) polymerization<sup>1,2</sup> has attracted great interest during recent years because it enables the formation of polymeric materials with controlled molecular weights, low polydispersities, and complex macromolecular architectures, such as block, comb, star, and hyperbranched (co)polymers. It is especially the matchless versatility of the RAFT process with respect to the type of monomer and the reaction medium that makes it a powerful method for generating novel materials with unrivalled properties. The mediating compounds employed in most RAFT polymerizations are dithioesters, Z-C(=S)S-R, which have been developed in great structural variety with respect to their leaving R-groups and to their stabilizing Z-moieties.<sup>3,4</sup> Effective RAFT agents include, e.g., dithiobenzoates, dithioacetates, dithiocarbonates (xanthates), and trithiocarbonates. RAFT polymerization proceeds via a degenerative chain transfer mechanism in which two equilibria (see Scheme 1) are superimposed onto a conventional radical polymerization scheme<sup>5</sup> with the elementary steps, i.e., of initiation, propagation, and termination, being unaffected. In the so-called preequilibrium, the addition of a propagating radical to the sulfur–carbon double bond of the RAFT agent **1** produces a carbon-centered intermediate RAFT radical **2**, which may undergo a  $\beta$ -scission reaction either yielding back the reactants or releasing an initiating radical R<sup>•</sup> plus a polymeric dithioester compound **3** that constitutes the dormant species. A similar set of reactions is operating in the main equilibrium, in which a growing macroradical reacts with the polymeric RAFT agent **3**. Repeated reversible addition fragmentation chain transfer events establish an equilibrium between dormant and living

## Scheme 1. Basic Reaction Steps of the Reversible Addition Fragmentation Chain Transfer (RAFT) Process

Pre-equilibrium:



Main equilibrium:



chains, resulting in the living/controlled characteristics of the polymerization.

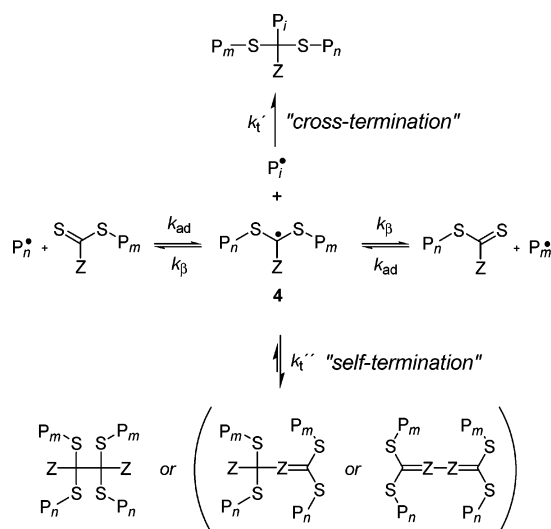
In addition to the developing synthetic applications of the RAFT process, much work has been directed toward a profound understanding of its mechanism and kinetics, which, however, has not been attained to a satisfactorily extent so far.<sup>6,7</sup> Knowledge of the fundamental reaction scheme is, however, mandatory to establish structure–rate correlations for a specific RAFT agent which information is essential for rational RAFT agent design delivering novel mediating compounds.

A variety of advanced techniques were applied to elucidate the detailed mechanism of RAFT polymerization and to arrive at rate coefficients describing the RAFT equilibrium reactions.<sup>8–15</sup> The choice of the RAFT reaction scheme used for data analysis has a significant impact on the rate coefficients obtained for the RAFT equilibrium. Special interest has focused on the question of whether irreversible termination reactions of the intermediate radical needs to be considered<sup>15</sup> or may be neglected.<sup>10</sup>

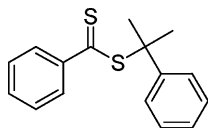
When employing dithiobenzoates, which are very effective RAFT agents,<sup>4</sup> inhibition (i.e., an initial time

\* Corresponding author. E-mail: pvana@uni-goettingen.de.

**Scheme 2. Modified Reversible Addition Fragmentation Chain Transfer (RAFT) Reaction Scheme Including Irreversible and Reversible Termination of the Intermediate RAFT Radical**



**Scheme 3. Cumyl Dithiobenzoate (CDB)**



period without any polymerization activity) and rate retardation (i.e., a decrease in the overall rate of polymerization with increasing initial RAFT agent concentration) are commonly observed, with the extent of both of these effects depending on the particular monomer system under investigation. Such kinetic effects provide valuable information about the RAFT mechanism because they constitute deviations from the ideal RAFT process, in which the propagating radical concentration, and hence the overall rate of polymerization, remains unchanged as compared to conventional polymerization. It is still unclear whether terminating side reactions of the intermediate radicals<sup>7,16</sup> (see Scheme 2) or extremely slow fragmentation of these species<sup>6</sup> is the fundamental cause of the rate retarding effect. However, it has generally been accepted that the relative stability and thus the average lifetime of the intermediate RAFT radicals **2** and **4** are of key importance for rate retardation and inhibition effects in RAFT polymerization.<sup>15</sup> Following either description of the RAFT process rate retardation is enhanced by an increased relative stability of the intermediate radical.

Recently we found that applying high pressure up to 2.5 kbar in cumyl dithiobenzoate (CDB, see Scheme 3) mediated RAFT polymerization of styrene improves the chain-length control and enhances the rate of polymerization.<sup>17</sup> Surprisingly, the relative change of the polymerization rate with varying RAFT agent concentration was independent of the applied pressure, indicating that the intermediate radical stability is not changed with pressure. This was unexpected because the addition reaction of the propagating radical toward the CDB was envisaged to be enhanced with increasing pressure, whereas the fragmentation reaction of the intermediate, yielding back a growing macroradical and a dithioester compound, may be suppressed.

Possible explanations for the independency of rate retardation on pressure included that (i) the addition

reaction, described by  $k_{ad}$ , is very fast and may become diffusion-controlled so that pressure may retard both  $k_{ad}$  and  $k_{\beta}$  and (ii) the increase of the stability of the intermediate radical may be compensated by a decrease of its termination rate, which may be suppressed to a larger extent than the reaction between two macroradicals.

To expand our investigations into the rate retardation effect, we studied the influence of increasing temperature and performed CDB-mediated styrene polymerization up to 180 °C and determined full molecular weight distributions of the resulting polymer and rate of polymerization data. So far, no systematic study into the effect of temperature on the course of a RAFT polymerization has been reported. Increasing temperature, in principle, favors the decomposition pathway of chemical reactions in comparison to addition reactions because of the corresponding entropy term. By applying high temperature, the fragmentation of the intermediate RAFT radical into the dithioester moiety and the propagating radical may therefore be enhanced compared to the addition reaction, by which the concentration of intermediate radicals is reduced and thus rate retardation is suppressed. High-temperature conditions, however, have also potential drawbacks for conducting controlled RAFT polymerizations; i.e., side reactions may generally be accelerated, and the dithioester moiety itself may undergo decomposition reactions, gradually reducing molecular weight control in the polymerizing system. To compensate for these disadvantages, we applied high pressure (1000 bar), which accelerates the polymerization rate and improves the molecular weight control, as we demonstrated earlier,<sup>17</sup> but should not affect the liquid properties significantly as the compressibility is low.

The present paper studies the RAFT process under high-temperature conditions, which may also be of technical interest, and probes whether CDB is a suitable mediating agent for conferring living characteristics on styrene polymerization under high-temperature conditions up to 180 °C. In addition, we aim at getting further insight into the kinetics and mechanism of the RAFT process via determining the rate retardation effect at such elevated temperatures.

## Experimental Part

Styrene (99%, Merck-Schuchardt) was purified by passing through a column filled with basic  $\text{Al}_2\text{O}_3$ . The RAFT agent CDB was synthesized according to the procedure detailed earlier.<sup>18</sup> The purity of CDB was better than 98% as verified by  $^1\text{H}$  NMR analysis. Tetrahydrofuran used as the eluent in size-exclusion chromatography (THF, Carl Roth, Rotipuran, stabilized with 2,6-di-*tert*-butyl-4-methylphenol), methanol (Fluka, p.a.), and hydroquinone (Merck-Schuchardt) were used as received.

All the reactions conducted in this study were bulk polymerizations without initiator; that is, they were thermally self-initiated by styrene. Initial monomer concentrations,  $[\text{M}]_0$ , were calculated from the  $p$ - $V$ - $T$  relation of styrene.<sup>19</sup> Initial monomer concentrations were between 8.0 and 8.9 mol  $\text{L}^{-1}$  depending on temperature. Polymerization temperatures were 120, 150, and 180 °C, and the applied pressure was 1000 bar. The initial concentrations of CDB were  $0, 5 \times 10^{-3}, 1.0 \times 10^{-2}$ , and  $2.0 \times 10^{-2}$  mol  $\text{L}^{-1}$ .

The experimental setup for preparing the reaction mixtures consisting of monomer and CDB was as follows. The major components were a pressure intensifier, a glass vessel for  $\text{CO}_2$  bubbling, a strain pressure gauge, and an optical high-pressure cell. Before introducing the reaction mixture into the pressure

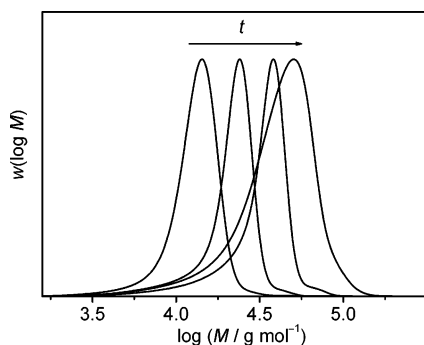


**Figure 1.** Time evolution of the normalized chain-length distribution (size-exclusion chromatography curves) in a cumyl dithiobenzoate-mediated ( $[\text{RAFT}]_0 = 1.0 \times 10^{-2} \text{ mol L}^{-1}$ ) self-initiated styrene bulk polymerization at  $150^\circ\text{C}$  and 1000 bar; samples are taken after 4, 10, 21, and 120 min with the associated monomer conversions being 10, 17, 32, and 61%, respectively.

intensifier, dissolved oxygen was eliminated by  $\text{CO}_2$  bubbling. By means of the pressure intensifier, the initial reaction mixture was fed into the optical high-pressure cell of transmission type equipped with two sapphire windows and pressurized to the desired pressure. The cell was subsequently disconnected from the pressure branch and inserted into the sample compartment of a Fourier transform IR/NIR spectrometer (IFS 88, Bruker). NIR spectra were recorded using a tungsten halogen lamp, a silicon-coated  $\text{CaF}_2$  beam splitter, and a liquid nitrogen cooled InSb detector. Monomer conversion as a function of time was determined from NIR spectra taken in the region of the C–H stretching first overtones at around  $6135 \text{ cm}^{-1}$ . To stop the polymerization after a predetermined time interval, the reaction solution was poured into methanol containing a small amount of hydroquinone. The polymer was collected after evaporating off residual monomer and methanol.

Molecular weight distributions were determined by size-exclusion chromatography using a Waters 515 HPLC pump, three PSS–SDV columns with nominal pore sizes of  $10^5$ ,  $10^3$ , and  $10^2 \text{ \AA}$ , a Waters 2410 refractive index detector, and THF at  $35^\circ\text{C}$  as the eluent with a flow rate of  $1.0 \text{ mL min}^{-1}$ . The SEC setup was calibrated against polystyrene (PS) standards of narrow polydispersity from Polymer Standards Service.

## Results and Discussion

CDB-mediated styrene bulk polymerizations were performed at temperatures of 120, 150, and  $180^\circ\text{C}$  at 1000 bar without initiator, and the full molecular weight distributions, MWD, as well as the rates of polymerization,  $R_p$ , were determined.

**Molecular Weight Distributions.** In living/controlled radical polymerization, the molecular weight of the resulting polymer increases steadily with reaction time and linearly with monomer conversion. Examining the molecular weight vs monomer conversion data thus provides information about the livingness of the process. As an example, Figure 1 depicts the evolution of the MWD of polystyrene with polymerization time,  $t$ , for a CDB-mediated polymerization at  $150^\circ\text{C}$  and 1000 bar, using a CDB concentration of  $1.0 \times 10^{-2} \text{ mol L}^{-1}$ . The reaction times are 4, 10, 21, and 120 min, corresponding to monomer conversions of 10, 17, 32, and 61%, respectively. The chain length of the generated polymer increases with reaction time, which indicates a controlled polymerization process. However, the molecular weight distribution after high monomer conversions exhibits a broadening, and a high molecular weight shoulder at twice the chain length of the peak molecular weight, which is due to the termination of propagating radicals via combination, occurs (Figure 1).

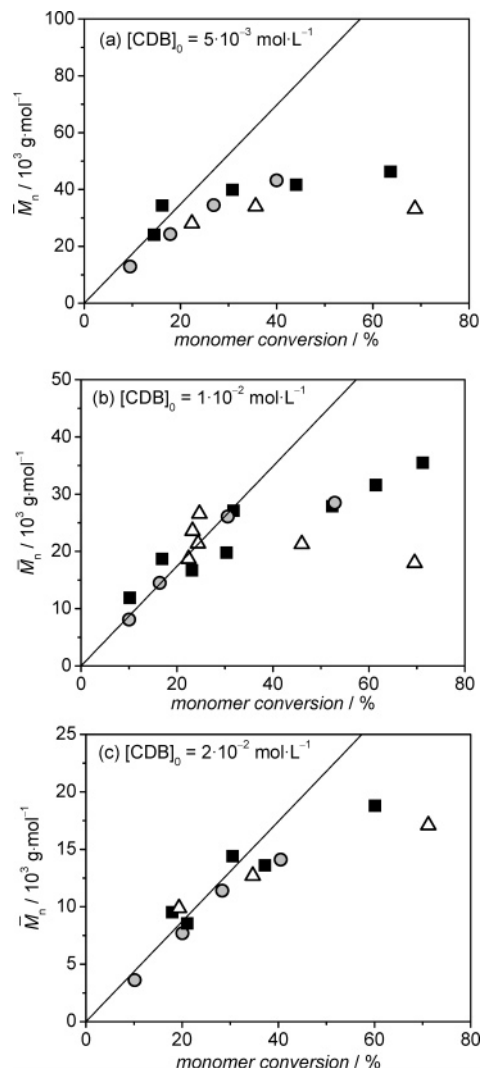


**Figure 2.** Number-average molecular weight,  $\bar{M}_n$ , vs monomer conversion for cumyl dithiobenzoate-mediated self-initiated styrene bulk polymerizations at 1000 bar at (○)  $120^\circ\text{C}$ , (■)  $150^\circ\text{C}$ , and (Δ)  $180^\circ\text{C}$  and using (a)  $5.0 \times 10^{-3}$ , (b)  $1.0 \times 10^{-2}$ , and (c)  $2.0 \times 10^{-2} \text{ mol L}^{-1}$  of RAFT agent. The straight lines indicate the respective theoretical number-average molecular weight according to eq 2.

The variation of the number-average molecular weight,  $\bar{M}_n$ , of the generated polymeric material with monomer conversion during the RAFT-controlled styrene polymerizations at temperatures of 120, 150, and  $180^\circ\text{C}$  and using CDB concentrations of  $5.0 \times 10^{-3}$ ,  $1.0 \times 10^{-2}$ , and  $2.0 \times 10^{-2} \text{ mol L}^{-1}$  is shown in Figure 2.

The experimental  $\bar{M}_n$  values increase with monomer to polymer conversion in the initial stage of RAFT polymerization at all investigated temperatures and then exhibit a downward deviation from the theoretical molecular weight values (full lines in Figure 2) that have been calculated via eq 1.

$$\bar{M}_n = \frac{X[M]_0 M_{\text{monomer}}}{[\text{RAFT}]_0} + M_{\text{RAFT}} \quad (1)$$

with the fractional monomer conversion,  $X$ ,  $[M]_0$  being the initial monomer concentration,  $[\text{RAFT}]_0$  being the initial CDB concentration, and  $M_{\text{monomer}}$  and  $M_{\text{RAFT}}$  being the molecular weights of the monomer and the RAFT agent, respectively. In eq 1, a constant number

of polymeric chains is assumed; that is, it describes the evolution of molecular weight in an ideal living polymerization.

Each data point presented in Figure 2 originates from an individual experimental run because taking samples during the polymerization is not easily carried out under high-pressure conditions. The extension of the monomer conversion regime in which ideal molecular weight control is exerted on the system depends on the initial RAFT agent concentration; i.e., when employing  $2 \times 10^{-2} \text{ mol L}^{-1}$  of CDB, the theoretical molecular weight values calculated by eq 1 are obtained up to almost 40% of monomer conversion at all temperatures, whereas deviations from molecular weight data predicted by eq 1 occur from 20% monomer conversion on when using  $5 \times 10^{-3} \text{ mol L}^{-1}$  of RAFT agent. Negative deviations from theoretical molar masses have already been observed in earlier studies into CDB-mediated styrene polymerizations both in toluene and in supercritical  $\text{CO}_2$ , where molecular weight control gradually decreased upon lowering CDB concentration.<sup>20</sup> Such an effect can be attributed to the continuous initiation process, which (i) yields small radicals that generate low molecular weight polyRAFT species via the RAFT equilibrium reactions (see Scheme 1) and (ii) propels the formation of dead polymeric material via conventional termination. Especially at high initiation rates, as is the case in self-initiated styrene polymerization at elevated temperature, and after substantial reaction times, the amount of chains derived by the initiation process cannot be ignored in comparison to the number of living chains. By accounting for polymeric chains produced via initiation in eq 1, the theoretical number-average molecular weight is therefore described by eq 2.<sup>21</sup>

$$\bar{M}_n = \frac{X[M]_0 M_{\text{monomer}}}{[\text{RAFT}]_0 + \frac{d}{2} \int_0^t R_i dt} + M_{\text{RAFT}} \quad (2)$$

with  $d$  being the number of chains that are generated in the termination process ( $d \approx 1$  for styrene) and  $R_i$  being the rate of initiation. The denominator of eq 2 represents the total concentration of polymeric chains, which is steadily increasing with reaction time  $t$ . The  $\bar{M}_n$  value of the polymeric material is hence a function of both monomer conversion and reaction time and exhibits lower values than that predicted by eq 1. The deviation from ideality, signified by a downward curvature of the  $\bar{M}_n$  vs  $X$  curve, is large at high initiation rates and becomes more prominent at increasing reaction times (see eq 2).

Evaluation of theoretical molecular weights according to eq 2 is not feasible in the present work because  $R_i$  in self-initiated styrene polymerization as a function of monomer conversion at the studied temperatures and 1000 bar is not accurately known. The experimental  $\bar{M}_n$  data are, however, in good qualitative agreement with the expected behavior predicted by eq 2. Smaller deviations from the straight line (Figure 2) in polymerizations using higher RAFT agent concentration are in agreement with the assumption that the observed downward curvatures are due to a high concentration of initiating radicals. The stronger deviations from the straight lines at higher temperature (Figure 2) are additionally in good accordance with an increasing initiation rate with increasing temperature.

To eliminate the influence of initiator-derived radicals on the average molecular weight, we plotted the peak

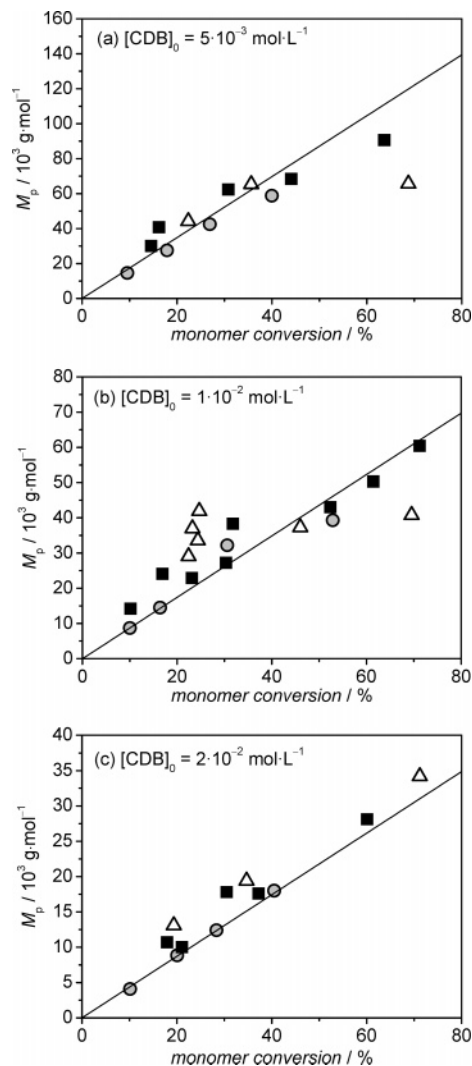


**Figure 3.** Peak molecular weight,  $M_p$ , vs monomer conversion for cumyl dithiobenzoate-mediated self-initiated styrene bulk polymerizations at 1000 bar at (○) 120, (■) 150, and (△) 180 °C and using (a)  $5.0 \times 10^{-3}$ , (b)  $1.0 \times 10^{-2}$ , and (c)  $2.0 \times 10^{-2} \text{ mol L}^{-1}$  of RAFT agent. The straight lines indicate the respective theoretical number-average molecular weight according to eq 2.

molecular weight,  $M_p$ , against  $X$  (Figure 3). The  $M_p$  value provides a good representation of the molecular weight of the living polymeric material that was initiated at the beginning of the controlled polymerization; hence, it is assumed to be very close to the ideal theoretical  $\bar{M}_n$ .<sup>20</sup> The  $M_p$  values show very good agreement with the ideal  $\bar{M}_n$  data calculated by eq 1 (full lines in Figure 3), indicating that the process retains livingness independent of temperature and RAFT agent concentration. The fraction of living chains, however, which can be estimated by dividing experimental  $\bar{M}_n$  data with theoretical values calculated via eq 1, can drop to a minimum of 30% in the case of high conversion and low RAFT agent concentration (Figure 2a).

Molecular weight control, i.e., increasing  $\bar{M}_n$  with  $X$ , is only slightly affected by increasing temperature. Only for the experiments at 180 °C with  $5.0 \times 10^{-3}$  and  $1.0 \times 10^{-2} \text{ mol L}^{-1}$  CDB (triangle symbols in Figure 2) is it difficult to decide whether the molecular weight systematically increases at low monomer conversions because of the rapid rate of polymerization at such conditions that does not allow for collecting samples easily at relatively low  $X$ . However, inspection of Figure

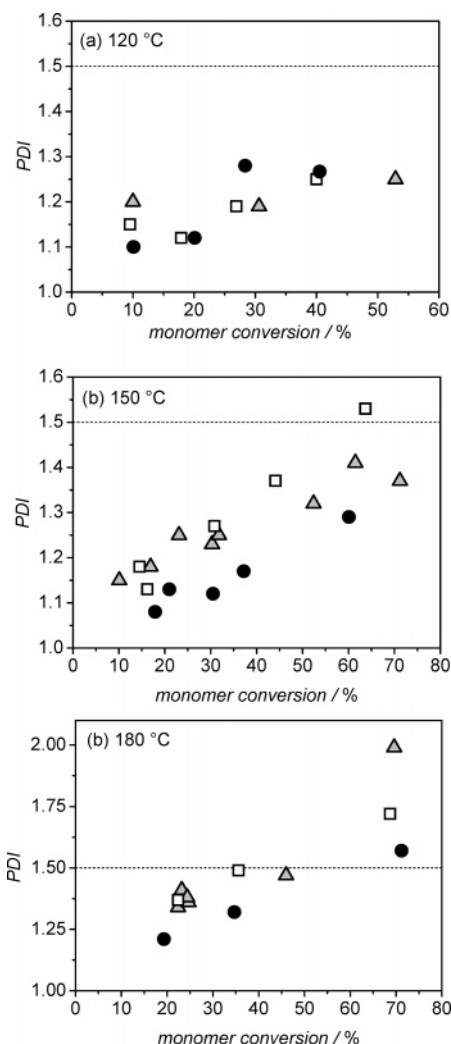


**Figure 4.** Polydispersity index, PDI, vs monomer conversion for cumyl dithiobenzoate-mediated self-initiated styrene bulk polymerizations at 1000 bar using ( $\square$ )  $5.0 \times 10^{-3}$ , ( $\triangle$ )  $1.0 \times 10^{-2}$ , and ( $\bullet$ )  $2.0 \times 10^{-2}$  mol L $^{-1}$  of RAFT agent at (a) 120, (b) 150, and (c) 180 °C.

4, which presents the polydispersity index (PDI) data of the individual polymerization series vs  $X$  are presented, indicates that the polydispersity of the samples generated at 180 °C are below 1.5 for monomer conversions below  $\sim 50\%$ , independently of the RAFT agent concentration. PDI values below the threshold value of  $\text{PDI} = 1.5$ , which marks the lowest PDI value that is accessible via conventional free-radical polymerization, are additional evidence for controlled polymerization being operative. The PDI values increase with monomer conversion at all investigated temperatures (Figure 4), which is due to the cumulative production of dead polymeric material as well as to the continuous generation of small radicals by the initiation process, which gradually increases the polydispersity of the final polymeric material. The polydispersity of the polymer generated via CDB-mediated styrene polymerization at 120 °C ranges from 1.1 to 1.3 for all employed RAFT agent concentrations, whereas PDI for polymerizations at 150 °C varies between 1.15 at low and 1.55 at high monomer conversion. The evolution of the PDI at 180 °C follows the same trend of polydispersity increasing with monomer conversion. Absolute PDI values at 180 °C are higher than at 150 °C and are in the range 1.2–2.0. At all experimental temperatures a slight tendency

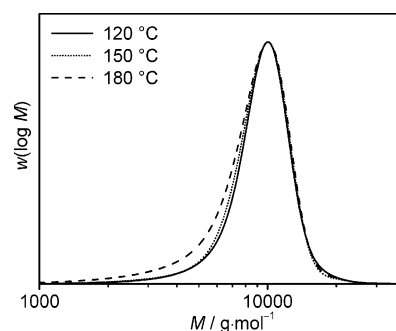


**Figure 5.** Normalized chain-length distributions (size-exclusion chromatography curves) from cumyl dithiobenzoate-mediated ( $[\text{RAFT}]_0 = 2.0 \times 10^{-2}$  mol L $^{-1}$ ) self-initiated styrene bulk polymerizations at 1000 bar and different reaction temperatures. Monomer conversion is close to 21%.

of decreasing PDI with increasing initial RAFT agent concentration is seen. The effect of increasing temperature, however, is found to be more prominent.

Figure 5 shows three polystyrene MWDs with nearly identical peak molecular weight from RAFT polymerizations to 21% monomer conversion at  $[\text{CDB}]_0 = 1.0 \times 10^{-2}$  mol L $^{-1}$ , 1000 bar, and temperatures of 120, 150, and 180 °C. Because of styrene self-initiation,<sup>22</sup> which is largely enhanced with increasing temperature, the initiation rate could not be kept constant for experiments at different temperatures. Consequently, the MWDs became broader with increasing temperature due to an elevated overall concentration of radicals which increases the rate of termination. Apparently, the MWD from the experiment at 180 °C is significantly broader. It is, however, difficult to decide whether the peak width increases upon elevating temperature from 120 to 150 °C because possible small changes may be hidden by the broadening occurring in the size-exclusion chromatography. The increasing amount of low-molecular-weight polymer material toward higher temperature enhances the PDI, as is obvious from Figure 4. Although causing a somewhat increased polydispersity in CDB-mediated styrene polymerization—mainly because of rapid initiation—very high temperatures do not deteriorate the molecular weight control itself, as indicated by Figure 2. If the control would suffer from increasing temperatures, the deviation of  $\bar{M}_n$  data from theoretical values according to eq 1 would occur at lower monomer conversions at elevated temperature conditions.

A first important result is that the RAFT process appears to be robust against elevated temperature conditions up to 180 °C as is evident from the increase in molecular weight with monomer conversion and from the polydispersities being below 1.5 (for the full monomer conversion regime at 120 °C, for  $X < 80\%$  at 150 °C and for  $X < 50\%$  for 180 °C) in CDB-mediated self-initiated styrene polymerizations.

**Rate of Polymerization.** To assess the influence of the relatively high temperatures on the rate retardation effect in CDB-mediated styrene polymerization, the rate of polymerization,  $R_p$ , in the initial low-conversion regime was determined for different RAFT agent concentrations.  $R_p$  was obtained by linearly fitting the initial part of the monomer conversion vs time plots from FT-NIR spectroscopy.<sup>23</sup> Inhibition effects could not be detected because the rapid rate of polymerization at the high-temperature high-pressure conditions of the present study did not allow for accurate rate measurements at monomer conversion below 2%. From the close-

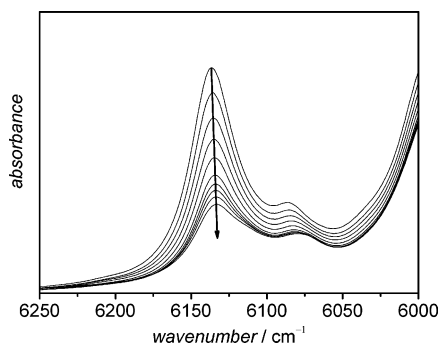


**Figure 6.** Series of NIR absorbance spectra taken during the course of a cumyl dithiobenzoate-mediated self-initiated styrene polymerization ( $[\text{RAFT}]_0 = 1.0 \times 10^{-2} \text{ mol L}^{-1}$ ) at 150 °C and 1000 bar up to styrene conversions of 62%.

to-linear part of the  $X$  vs  $t$  plots in the conversion range from about 2 to 15%, the polymerization rate,  $R_p = [M]_0 \Delta X / \Delta t$ , was estimated. The  $R_p$  data therefore refer to the reaction period after passing the preequilibrium stage and reaching stationary conditions. It should further be noted that  $R_p$  refers to the monomer conversion regime, in which the RAFT polymerizations proceed with good molecular weight control (see Figure 2). Figure 6 shows an NIR spectral series recorded during a spontaneous styrene polymerization (that is without adding an initiator) at 1000 bar and 150 °C using a CDB concentration of  $1.0 \times 10^{-2} \text{ mol L}^{-1}$ . The arrow indicates the direction of spectral change with polymerization time. The absorbance at around  $6136 \text{ cm}^{-1}$  reflects the depletion of monomer.

To quantify the rate-retarding effect of increasing RAFT agent concentration in CDB-mediated styrene polymerization, the  $R_p$  data are plotted on a semilogarithmic graph vs initial RAFT agent concentration,  $[\text{RAFT}]_0$ , in Figure 7. Such plots yield close-to-linear correlations for styrene polymerizations mediated by dithiobenzoates and trithiocarbonates.<sup>24</sup> The rate retardation parameter,  $\rho$ , which may be evaluated from such plots via

$$\rho = - \frac{d \ln(R_p / (\text{mol L}^{-1} \text{ s}^{-1}))}{d[\text{RAFT}]_0} \quad (3)$$

also served for quantification of rate retardation in our previous study into CDB-mediated styrene polymerizations in  $\text{CO}_2$ .<sup>20</sup> It should be noted that each  $R_p$  data point represents the average value over rate data from up to five individual RAFT experiments. Such multiple data sampling has become necessary because the experimental scatter of rate data was found to be enhanced in comparison to experiments at lower temperatures, which is due to rapid polymerization and the increasing difficulties of controlling temperature at the unusual reaction conditions of the present study.

Inspection of the  $R_p$  data in Figure 7 reveals two important features:

1. Absolute  $R_p$  is largely increased between 120 and 180 °C by a factor of about 30 for conventional styrene polymerization and by a factor of about 36 for the RAFT-controlled styrene polymerization using  $2 \times 10^{-2} \text{ mol L}^{-1}$  CDB. The fast rate of polymerization corresponds to 25% of initial monomer conversion within 3 min at 180 °C, 1000 bar, and  $1 \times 10^{-2} \text{ mol L}^{-1}$  of initial CDB. Under these polymerization conditions the molecular

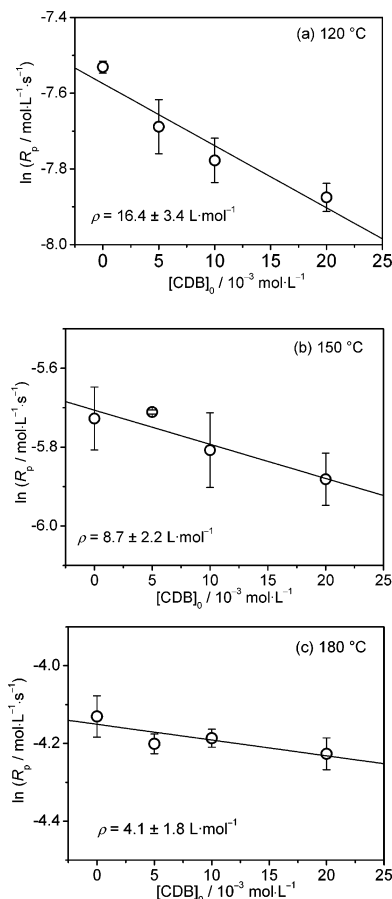


**Figure 7.** Semilogarithmic plot of the rate of polymerization,  $R_p$ , for the conversion range from 2 to 15% (see text), vs initial RAFT agent concentration,  $[\text{CDB}]_0$ , for cumyl dithiobenzoate-mediated self-initiated styrene polymerizations at 1000 bar and at (a) 120, (b) 150, and (c) 180 °C. The error bars indicate the standard deviation of the individual experimental data points. The slope of the best linear fits (straight lines), i.e., the rate retardation parameter,  $\rho$ , is indicated in the figures.

weight is still controlled, and polydispersities of about 1.3 are obtained.

2. The impact of RAFT agent concentration on  $R_p$  decreases toward increasing temperature. The rate retardation parameter, e.g., drops from  $16.4 \text{ L mol}^{-1}$  at 120 °C over  $8.7 \text{ L mol}^{-1}$  at 150 °C to  $4.1 \text{ L mol}^{-1}$  at 180 °C. In preceding work on the same system at 80 °C and 300 bar,  $\rho$  has been found to be  $27.9 \text{ L mol}^{-1}$ ,<sup>20</sup> which number is consistent with the  $\rho$  values reported here. It should be noted that the entire set of  $\ln R_p$  vs  $[\text{CDB}]_0$  plots is close to linear. This, however, has no mechanistic implications since the retardation parameter is a purely empirical quantity.

The decreasing rate retardation effect toward higher temperature may be understood by a shift of the RAFT equilibrium toward lower equilibrium concentrations of the intermediate RAFT radicals, as has been put forward in the Introduction section. The alternative explanation which assumes that RAFT agent decomposition provides additional initiation, thus compensating for rate retardation at increasing RAFT agent concentration, cannot be definitely ruled out. This latter explanation, however, appears to be unlikely for the following reasons: (i) The loss of RAFT agent concentration that would be associated with radical production from CDB should result in a deviation of experimental  $\bar{M}_n$  from theoretical  $\bar{M}_n$  to higher values, which is not

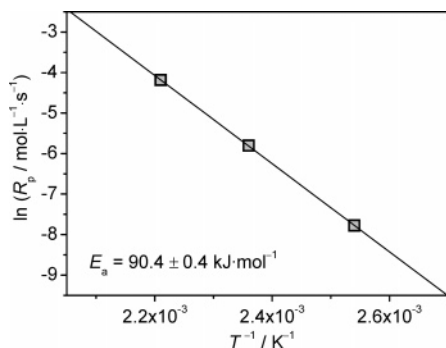


**Figure 8.** Arrhenius plot of the overall rate of polymerization,  $\ln R_p$ , for a cumyl dithiobenzoate-mediated ( $[\text{RAFT}]_0 = 1.0 \times 10^{-2} \text{ mol L}^{-1}$ ) self-initiated styrene bulk polymerization at 1000 bar.

observed. (ii) The dithioester moiety is not prone to thermally induced homolytic bond breakage yielding radicals, as CDB lacks the typical features of radical initiator molecules, such as bonds between heteroatoms or subunits that may be eliminated thereby producing stable species. Dithioesters are more likely to decompose thermally by desulfurization via ionic rearrangement reactions.<sup>25</sup> (iii) Unimolecular fragmentation reactions delivering radicals, such as initiator decomposition, are known to exhibit substantial activation energies of more than  $100 \text{ kJ mol}^{-1}$ , rendering the temperature range in which continuous radical production occurs limited. The observed rate retardation effect, however, smoothly decreases over the temperature range  $80 \text{ }^\circ\text{C}^{20}$  to  $180 \text{ }^\circ\text{C}$ , in which a classical bond breaking to produce radicals would be accelerated by more than 3 orders of magnitude.

Decomposition of the RAFT agent at very high temperatures may induce ionic polymerization processes, impeding the controlling RAFT process. We made an Arrhenius-type plot of  $R_p$  for the CDB-mediated styrene polymerization with  $[\text{CDB}]_0 = 2.0 \times 10^{-2} \text{ mol L}^{-1}$  (Figure 8) to check whether there are indications of any change in reaction mechanism within the experimental temperature range. The  $\ln R_p$  vs  $1/T$  graph exhibits almost perfect linearity with an associated activation energy of  $90.4 \pm 0.4 \text{ kJ mol}^{-1}$ . This linearity suggests that no change in reaction mechanism occurs toward increasing temperature. Linear Arrhenius plots as in Figure 8 were also observed at the other experimental RAFT agent concentrations. Contributions to polymerization activity by ionic processes may therefore be ruled out for the entire set of RAFT polymerization conditions employed within the present study.

Our rate data have also been analyzed via eq 4, which has been provided by the Fukuda group,<sup>9</sup> for RAFT polymerization rate,  $R_p$ , for the situation of intermediate radicals terminating irreversibly either by reaction with propagating macroradicals or by self-termination (see Scheme 2)

$$R_p = R_{p,c} \{1 + 2(k_t'/k_t)K[\text{RAFT}]_0 + (k_t''/k_t)K^2[\text{RAFT}]_0^2\}^{-0.5} \quad (4)$$

with  $R_{p,c}$  being the conventional polymerization rate (without RAFT agent),  $k_t$  being the termination rate coefficient for the reaction between two propagating radicals,  $k_t'$  being the cross-termination rate coefficient for the combination reaction of an intermediate RAFT radical with a growing macroradical,  $k_t''$  denoting the

self-termination rate coefficient of two intermediate RAFT radicals, and  $K$  being the RAFT equilibrium constant,  $K = k_{ad}/k_{\beta}$ . Reversible termination reactions of the intermediate RAFT radicals are not accounted for in eq 4 and that the loss of dithioester groups due to irreversible termination reactions of the intermediate RAFT radical is neglected.

The analytical description of  $R_p$  via eq 4 further assumes that stationary conditions are established. Although it has not been proven that irreversible termination reactions of the intermediate radical are the single reason for the rate retardation effect, eq 4 is used in this study because this is the only analytical expression for  $R_p$  as a function of RAFT agent concentration that is currently available. Alternatively hypothesized causes for rate retardation are, e.g., stable intermediate RAFT radicals<sup>6</sup> or reversible termination<sup>26,27</sup> of these species. Such reactions result in nonstationary polymerization conditions, which currently impede any analytical description of RAFT polymerization rates because of the complex and coupled reaction scheme.

It has been reported that the rate retardation effect in CDB-mediated styrene bulk polymerization may be adequately described by only taking cross-termination reactions of intermediate radicals with propagating radicals into account,<sup>9,28</sup> whereby eq 4 reduces to

$$R_p^{-2} = R_{p,c}^{-2} \{1 + 2(k_t'/k_t)K[\text{RAFT}]_0\} \quad (5)$$

where self-termination between two intermediate radicals is assumed to be not significant. This assumption for the kinetic analysis is even more valid at high-temperature conditions, where the concentration of the intermediate radicals is envisaged to be reduced. Experimental rate data for constant polymerization temperature may be fitted as  $R_p^{-2}$  vs  $[\text{RAFT}]_0$  to yield  $(k_t'/k_t)K$  from the linear slope of such plots. The resulting  $(k_t'/k_t)K$  values may also serve as a measure for the rate retardation effect. The information on the equilibrium constant,  $K$ , may be correlated with the stability and the concentration of intermediate RAFT radicals.

Shown in Figure 9 are the  $R_p^{-2}$  vs  $[\text{CDB}]_0$  plots for CDB-mediated styrene polymerizations at 120, 150, and  $180 \text{ }^\circ\text{C}$ . The data for each individual temperature may be fitted to eq 5, which is consistent with that cross-termination constitutes the main cause of rate retardation, irrespective of temperature, and that self-termination between two intermediate radicals does not occur to any appreciable extent, as has also been observed for CDB-mediated methyl acrylate polymerization.<sup>28</sup>

The slopes of the straight lines in Figure 9 yield  $(k_t'/k_t)K$  values of  $22.3 \text{ L mol}^{-1}$  at  $120 \text{ }^\circ\text{C}$ ,  $10.7 \text{ L mol}^{-1}$  at  $150 \text{ }^\circ\text{C}$ , and  $4.3 \text{ L mol}^{-1}$  at  $180 \text{ }^\circ\text{C}$ , again reflecting the alleviated rate retardation effect when increasing reaction temperature. It should be noted that the  $(k_t'/k_t)K$  value of  $54 \text{ L mol}^{-1}$ , which we reported recently for  $80 \text{ }^\circ\text{C}$ ,<sup>28</sup> fits very well to the temperature dependence of this coupled parameter but has not been incorporated in the present data analysis because it was evaluated from a slightly different system, that is, at 300 bar and with 22 vol % of toluene as a solvent.

Plotting the  $(k_t'/k_t)K$  data in an Arrhenius-type graph (Figure 10) allows for deducing the activation energy of this coupled parameter:  $E_a((k_t'/k_t)K) = -40.5 \text{ kJ mol}^{-1}$ . This overall activation energy is composed of the

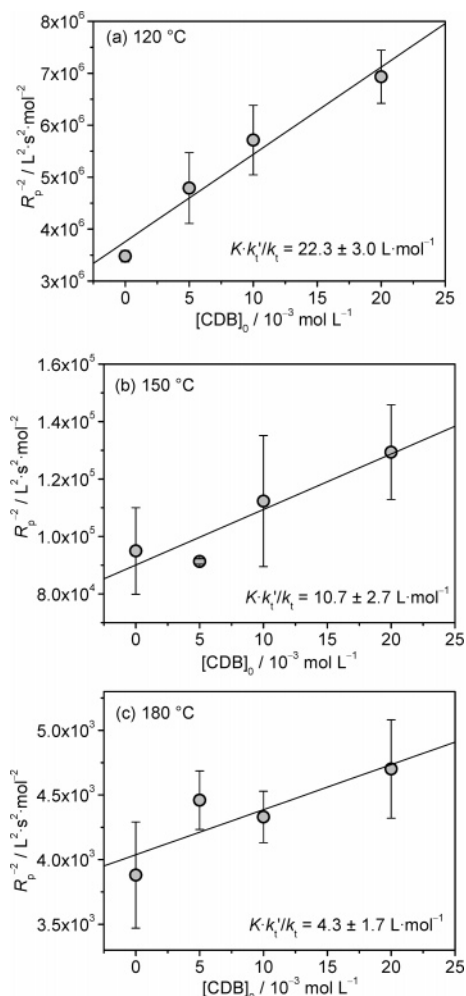


**Figure 9.** Plot of squared inverse rate of polymerization,  $R_p^{-2}$ , vs RAFT agent concentration,  $[CDB]_0$ , for cumyl dithiobenzoate-mediated self-initiated styrene polymerizations at 1000 bar and (a) 120, (b) 150, and (c) 180 °C. The  $Kk_t'/k_t$  values, evaluated from the slope of the linear fits (see eq 5), are indicated in the figures.

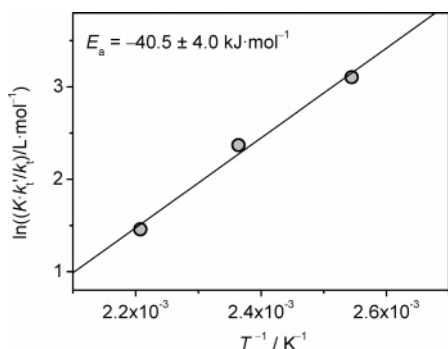


**Figure 10.** Arrhenius plot of  $\ln(Kk_t'/k_t)$  for the cumyl dithiobenzoate-mediated self-initiated styrene bulk polymerization at 1000 bar. The corresponding activation energy, evaluated from the best linear fit, is indicated in the figure.

activation energies of the individual rate coefficients according to eq 6:

$$E_a((k_t'/k_t)K) = E_a(k_t') - E_a(k_t) + E_a(k_{ad}) - E_a(k_\beta) \quad (6)$$

Radical–radical recombination or disproportionation reactions are known to be diffusion-controlled.<sup>29</sup> Their activation energy may be identified with the temperature dependence of the viscosity of the polymerization

system.<sup>30,31</sup> The activation energies of  $k_t$  and  $k_t'$  may thus be assumed to be very close to each other. In case that both energies are identical, eq 6 reduces to the subsequent simple expression, which correlates the activation energies of the two processes that determine the RAFT equilibrium constant (eq 7).

$$E_a(k_{ad}) - E_a(k_\beta) = -40.5 \text{ kJ mol}^{-1} \quad (7)$$

This difference in activation energies, to a good approximation, also represents the associated difference in activation enthalpies,  $\Delta H^\ddagger(\text{ad})$  and  $\Delta H^\ddagger(\beta)$ , respectively, and thus the reaction enthalpy,  $\Delta H$ , for the addition of polystyryl radicals to polystyryl dithiobenzoate (polyRAFT) intermediate species.

$$\Delta H^\ddagger(\text{ad}) - \Delta H^\ddagger(\beta) = \Delta H \approx -40.5 \text{ kJ mol}^{-1} \quad (8)$$

The so-obtained approximate reaction enthalpy is notably different from the corresponding  $\Delta H = -78 \text{ kJ mol}^{-1}$  value estimated via ab initio calculations for the addition reaction of cumyl radicals to methyl dithiobenzoate to yield  $\text{Ph}(\text{CH}_2)_2\text{C}-\text{S}-\text{C}^\bullet\text{Ph}-\text{S}-\text{CH}_3$ ,<sup>10</sup> which reaction is considered to mimic the preequilibrium reaction of CDB-mediated polymerization.

Ab initio calculations<sup>32</sup> suggested that the addition reactions of small radicals toward dithioesters yielding intermediate RAFT radicals occur almost barrierless; i.e.,  $\Delta H^\ddagger(\text{ad})$  is close to zero. Experimental studies into the activation energy of the polystyryl radical addition rate to polymeric dithioacetates<sup>33</sup> resulted in  $\Delta H^\ddagger(\text{ad})$  close to  $21 \text{ kJ mol}^{-1}$ . The arithmetic mean of these two values,  $\Delta H^\ddagger(\text{ad}) = 10.5 \pm 10.5 \text{ kJ mol}^{-1}$ , together with  $\Delta H^\ddagger(\text{ad}) - \Delta H^\ddagger(\beta) = -40.5 \text{ kJ mol}^{-1}$ , results in an activation enthalpy for the  $\beta$ -scission reaction of the intermediate RAFT radical of  $\Delta H^\ddagger(\beta) = 51.0 \pm 10.5 \text{ kJ mol}^{-1}$ . Using this barrier in conjunction with the pre-exponential factors deduced via transition-state theory<sup>32</sup> leads to a  $\beta$ -scission rate coefficient of about  $6 \times 10^3 \text{ s}^{-1}$  at 60 °C.

This  $k_\beta$  value is very close to the one of  $10^4 \text{ s}^{-1}$  which has been deduced for CDB-mediated styrene polymerization at 60 °C<sup>7</sup> by data evaluation, which was also based on the concept of irreversible termination of the intermediate radical, using, however, different experimental means, i.e., including ESR-spectroscopically determined radical concentrations. It is interesting to note that by using the *intermediate termination model* the CDB-mediated styrene polymerization can be described with remarkable internal consistency over the wide temperature range of 60–180 °C.

The temperature is less satisfactory when one assumes that absence of termination reactions of the intermediate RAFT radicals are not occurring. It needs to be noted that our experimental data are in disagreement with the alternative so-called *slow fragmentation model*,<sup>6,10</sup> which assigns the rate retardation effect exclusively to the high stability of intermediate radicals. Rate retardation in the *slow fragmentation model* results from nonstationary conditions during the entire period of polymerization, in which the high stability of intermediate radicals prevents reaching stationary propagating radical concentration.<sup>34</sup> For CDB-mediated styrene polymerization, equilibrium constants,  $K$ , of  $1.06 \times 10^7 \text{ L mol}^{-1}$  for 30 °C<sup>10</sup> and  $1.6 \times 10^7 \text{ L mol}^{-1}$  for 60 °C<sup>35</sup> were deduced via modeling kinetic data on the basis of the *slow fragmentation model*. These high  $K$  values are associated with a high activation enthalpy,  $\Delta H^\ddagger(\beta)$ , for

the  $\beta$ -scission reaction of the intermediate RAFT radical. Recent ab initio calculations predicted the reaction enthalpy for the addition of radicals to the dithiobenzoate intermediate RAFT species in the main equilibrium to be at least  $\Delta H = -78 \text{ kJ mol}^{-1}$ , which fits into the slow fragmentation picture.<sup>10</sup> Combining this value with the above-mentioned activation enthalpy for the addition step,  $\Delta H^+(\text{ad}) = 10.5 \pm 10.5 \text{ kJ mol}^{-1}$ , yields a fairly large activation enthalpy for the  $\beta$ -scission step of the intermediate RAFT species:  $\Delta H^+(\beta) = 88.5 \pm 10.5 \text{ kJ mol}^{-1}$ . An activation barrier of this size would be associated with an enormous increase of  $k_\beta$  with temperature, e.g., a  $k_\beta$  value of  $0.4 \text{ s}^{-1}$  at  $30^\circ\text{C}$ ,<sup>10</sup> would increase up to  $k_\beta = 1200 \text{ s}^{-1}$  at  $120^\circ\text{C}$ , resulting in a decrease of the equilibrium constant  $K$  by about 3 orders of magnitude. As a consequence of this lowering in  $K$ , the rate retardation effect would disappear at  $120^\circ\text{C}$ , as has been demonstrated in comprehensive simulations of the slow fragmentation model.<sup>34</sup>

The clearly observed rate retardation effect in CDB-mediated styrene polymerization at temperatures of  $120^\circ\text{C}$  and above thus is in conflict with a RAFT mechanism that assigns rate retardation effect entirely to slowly fragmentation of the intermediate radicals. Including irreversible termination of the intermediate RAFT radicals, on the other hand, allows for a consistent representation of the experimental rate data within the extended temperature range covered within the present study, thus proving strong support for the validity of this mechanistic concept.

## Conclusion

Cumyl dithiobenzoate mediated styrene polymerizations between  $120$  and  $180^\circ\text{C}$  proceeded with molecular weights increasing with monomer conversion and yielded polymer with polydispersity indices well below 1.5. No indications of a change in the overall RAFT polymerization process, e.g., by ionic side reactions, were found. Retardation of the polymerization rate with increasing RAFT agent concentration decreased with temperature and was clearly seen up to  $150^\circ\text{C}$ , which can be attributed to a lowered equilibrium concentration of intermediate RAFT radicals. The experimental rate data could consistently be described by the concept of irreversible termination of the intermediate RAFT radical but are in conflict with an interpretation that assumes very slowly fragmenting intermediate radicals being responsible for the rate retardation effect. The kinetic studies indicate that RAFT polymerizations at high temperatures may be of interest for technical applications because the rate of polymerization is dramatically increased by concomitantly retaining control over molecular weight.

**Acknowledgment.** Financial support by the Deutsche Forschungsgemeinschaft granted within the framework of the European Graduate School "Microstructural Control in Free-Radical Polymerization" is gratefully acknowledged.

## References and Notes

- Chiefari, J.; Chong, Y. K.; Ercole, F.; Krstina, J.; Jeffery, J.; Le, T. P. T.; Mayadunne, R. T. A.; Meijs, G. F.; Moad, C. L.; Moad, G.; Rizzardo, E.; Thang, S. H. *Macromolecules* **1998**, *31*, 5559–5562.
- Barner-Kowollik, C.; Davis, T. P.; Heuts, J. P. A.; Stenzel, M. H.; Vana, P.; Whittaker, M. J. *Polym. Sci., Part A: Polym. Chem.* **2003**, *41*, 365–375.
- Chong, Y. K.; Krstina, J.; Le, T. P. T.; Moad, G.; Postma, A.; Rizzardo, E.; Thang, S. H. *Macromolecules* **2003**, *36*, 2256–2272.
- Chiefari, J.; Mayadunne, R. T. A.; Moad, C. L.; Moad, G.; Rizzardo, E.; Postma, A.; Skidmore, M. A.; Thang, S. H. *Macromolecules* **2003**, *36*, 2273–2283.
- Vana, P.; Barner-Kowollik, C.; Davis, T. P.; Matyjaszewski, K. Radical Polymerization. In *Encyclopedia of Polymer Science and Technology*, 3rd ed.; Mark, H. F., Ed.; Wiley-Interscience: Hoboken, NJ, 2004; Vol. 11, pp 359–472.
- Barner-Kowollik, C.; Coote, M. L.; Davis, T. P.; Radom, L.; Vana, P. *J. Polym. Sci., Part A: Polym. Chem.* **2003**, *41*, 2828–2832.
- Wang, A. R.; Zhu, S.; Kwak, Y.; Goto, A.; Fukuda, T.; Monteiro, M. S. *J. Polym. Sci., Part A: Polym. Chem.* **2003**, *41*, 2833–2839.
- McLeary, J. B.; Calitz, F. M.; McKenzie, J. M.; Tonge, M. P.; Sanderson, R. D.; Klumperman, B. *Macromolecules* **2004**, *37*, 2383–2394.
- Kwak, Y.; Goto, A.; Fukuda, T. *Macromolecules* **2004**, *37*, 1219–1225.
- Feldermann, A.; Coote, M. L.; Stenzel, M. H.; Davis, T. P.; Barner-Kowollik, C. *J. Am. Chem. Soc.* **2004**, *126*, 15915–15923.
- Calitz, F. M.; Tonge, M. P.; Sanderson, R. D. *Macromolecules* **2003**, *36*, 5–8.
- Ah Toy, A.; Vana, P.; Davis, T. P.; Barner-Kowollik, C. *Macromolecules* **2004**, *37*, 744–751.
- Vana, P.; Quinn, J. F.; Davis, T. P.; Barner-Kowollik, C. *Aust. J. Chem.* **2002**, *55*, 425–431.
- Kwak, Y.; Goto, A.; Tsujii, Y.; Murata, Y.; Komatsu, K.; Fukuda, T. *Macromolecules* **2002**, *35*, 3026–3029.
- Drache, M.; Schmidt-Naake, G.; Buback, M.; Vana, P. *Polymer*, available online (doi: 10.1016/j.polymer.2004.11.117).
- Monteiro, M. J.; de Brouwer, H. *Macromolecules* **2001**, *34*, 349–352.
- Arita, T.; Buback, M.; Janssen, O.; Vana, P. *Macromol. Rapid Commun.* **2004**, *25*, 1376–1381.
- Perrier, S.; Barner-Kowollik, C.; Quinn, J. F.; Vana, P.; Davis, T. P. *Macromolecules* **2002**, *35*, 8300–8306.
- Kuchta, F.-D. PhD Thesis, University of Göttingen, Göttingen, 1996.
- Arita, T.; Beuermann, S.; Buback, M.; Vana, P. *e-Polym.* **2004**, *003*, 1–14.
- Moad, G.; Rizzardo, E.; Thang, S. H. *Aust. J. Chem.* **2005**, *58*, 379–410.
- Mayo, F. R. *J. Am. Chem. Soc.* **1968**, *90*, 1289–&.
- Buback, M. *Angew. Chem., Int. Ed. Engl.* **1991**, *30*, 641–653.
- Davis, T. P.; Barner-Kowollik, C.; Nguyen, T. L. U.; Stenzel, M. H.; Quinn, J. F.; Vana, P. *ACS Symp. Ser.* **2003**, *854*, 551–569.
- Scheithauer, S.; Mayer, R. *Thio- and Dithiocarboxylic Acids and Their Derivatives*; Georg Thieme Verlag: Stuttgart, 1979; p 225.
- Monteiro, M. J.; Bussels, R.; Beuermann, S.; Buback, M. *Aust. J. Chem.* **2002**, *55*, 433–437.
- Barner-Kowollik, C.; Quinn, J. F.; Nguyen, T. L. U.; Heuts, J. P. A.; Davis, T. P. *Macromolecules* **2001**, *34*, 7849–7857.
- Arita, T.; Beuermann, S.; Buback, M.; Vana, P. *Macromol. Mater. Eng.* **2005**, *290*, 283–293.
- Buback, M.; Egorov, M.; Gilbert, R. G.; Kaminsky, V.; Olaj, O. F.; Russell, G. T.; Vana, P.; Zifferer, G. *Macromol. Chem. Phys.* **2002**, *203*, 2570–2582.
- Benson, S. W.; North, A. M. *J. Am. Chem. Soc.* **1959**, *81*, 1339–1345.
- Mahabadi, H. K.; Odriscoll, K. F. *J. Polym. Sci., Part A: Polym. Chem.* **1977**, *15*, 283–300.
- Coote, M. L. *J. Phys. Chem. A* **2005**, *109*, 1230–1239.
- Goto, A.; Sato, K.; Tsujii, Y.; Fukuda, T.; Moad, G.; Rizzardo, E.; Thang, S. H. *Macromolecules* **2001**, *34*, 402–408.
- Vana, P.; Davis, T. P.; Barner-Kowollik, C. *Macromol. Theory Simul.* **2002**, *11*, 823–835.
- Barner-Kowollik, C.; Quinn, J. F.; Morsley, D. R.; Davis, T. P. *J. Polym. Sci., Part A: Polym. Chem.* **2001**, *39*, 1353–1365.